ISSN 1995-0780, Nanotechnologies in Russia, 2015, Vol. 10, Nos. 7–8, pp. 600–605. © Pleiades Publishing, Ltd., 2015.
Original Russian Text © K. Kvamen, S. Grigoryan, D.V. Anokhin, V.A. Bataev, A.I. Smirnov, D.A. Ivanov, 2015, published in Rossiiskie Nanotekhnologii, 2015, Vol. 10, Nos. 7–8.

In-situ Investigation of the Bulk Heterojunction Formation Processes in the Active Layers of Organic Solar Cells

K. Kvamen[a], S. Grigoryan[a], D. V. Anokhin[b,c], V. A. Bataev[d], A. I. Smirnov[d], and D. A. Ivanov[b,e]

[a] *Solid State Physics, University of Siegen, Walter Flex Strasse-3, D-57068 Siegen, Germany*

[b] *Faculty of Fundamental Physicochemical Engineering, Moscow State University, Moscow, 119991 Russia*

[c] *Institute of Problems of Chemical Physics, Russian Academy of Sciences, pr. Akademika Semenova 1, Chernogolovka, Moscow oblast, 142432 Russia*

[d] *Novosibirsk State Technical University, pr. Karla Marksa 20, Novosibirsk, 630073 Russia*

[e] *Institut de Sciences des Matériaux de Mulhouse, CNRS UMR 7361, 15, Jean Starcky, F-68057, Mulhouse, France*

e-mail: dimitri.ivanov@uha.fr

Received December 23, 2014; in final form, April 9, 2015

Abstract—Conjugated polymer-based organic photovoltaic devices (OPVs) have been intensively studied, since they are advantageous over regular inorganic devices. However, there is still no complete understanding of the functionality of conjugated polymer-based organic active layers. Due to this, research into the processes of microstructure formation will improve morphology control and optimization and enhance performance and productivity. In this study we used in situ measurements of conductivity and X-ray diffraction analysis in grazing incidence X-ray diffraction (GIXD) geometry to investigate the structure of light-sensitive layers produced by coating from solutions and based on poly(3-hexylthiophene) (P3HT) mixtures as donors with various fullerene acceptors: [6,6]-phenyl-C61 butyric acid methyl ester (PCBM) and indene-C60 bis-adduct (ICBA). The structure of films produced by coating from solutions was studied by large-angle GIXD. Ex situ and in situ methods (under external voltage applied) were used to detect high compatibility between the donor and acceptor for ICBA-based films. The time dependences of changes in current and intensity of the (100) peak of P3HT demonstrate that the maximum emerges simultaneously. A two-step increase in intensity of the (100) peak of P3HT was observed for films containing PCBM as an acceptor. In situ studies of the structure confirm that the joint donor–acceptor structure is formed as the solvent evaporates. Atomic force microscopy studies of the surface roughness of films containing different acceptors demonstrate that they are characterized by different morphologies.

Keywords: organic photovoltaic devices, in situ studies of the structure and electric properties, X-ray diffraction in grazing incidence X-ray diffraction geometry, polymer crystallization.

DOI: 10.1134/S1995078015040102

INTRODUCTION

Energy plays a crucial role in the development and maintenance of the society. The demand for energy increases annually with the increasing population, and this is particularly true for environmentally clean energy production [1]. Although there are many sources for generating clean renewable energy (wind power plants, geothermal and bioelectric power stations), solar energy is of particular interest [2]. Great focus has recently been placed over organic photovoltaic devices (OPVs) due to their numerous advantages over inorganic devices, such as low cost and simplicity of production [3]. Inexpensive organic solvents, such as chloroform ($CHCl_3$), chlorobenzene (CB), dichlorobenzene (DCB), toluene, etc., can be used to produce OPVs. Three different types of *pn*-junctions can be distinguished for OPVs. The simplest occurs in a single-layer OPV, where a layer of organic material is applied between two conductors (e.g., made of indium tin oxide (ITO)). The main problem of this junction is that electrons can easily recombine with holes, thus fail to reach electrodes. Multilayer OPVs were proposed to solve this problem. The first type includes bilayer OPVs with two different layers between the electrodes. Since mean free path of excitons in organic materials is limited (~10 nm) [4], they need to be formed near the surface to ensure diffusion. However, this criterion sometimes cannot be fulfilled in this type of OPV. OPVs with volume heterojunction allow one to solve this problem, since they offer a bicontinuous network of donor and acceptor pathways that are needed for charge carriers to be moved to electrodes. In an ideal situation, an OPV with volume heterojunction consists of electron-donor polymer mixed with electron-acceptor fullerene material. This system undergoes phase segregation, giving rise to a structure

consisting of mutually permeating grids between two electrodes. The effectiveness of their photoconversion increases with the absorptance of the polymer in the solar spectrum and degree of crystallinity of the polymer [5–7].

The system based on poly(3-hexylthiophene) (P3HT) as an electron donor and [6, 6]-phenyl-C61 butyric acid methyl ester (PCBM) as an electron acceptor with its performance being as high as ~5% is the best-studied system with bulk heterojunction [8]. Since donor material absorbs solar flux, its absorbance range is supposed to be as close to the solar spectrum as possible, which makes P3HT a suitable material as a donor (at wavelengths up to 650 nm). The new acceptor material, indene-C60 bis-adduct (ICBA), which is much easier to synthesize, is considered along with PCBM. Furthermore, it is more soluble in most solvents and has a higher extinction coefficient in the visible region of the spectrum compared to PCBM. The effectiveness of ICBA-based OPVs can be as high as ~6.5% [9]. The lowest unoccupied molecular orbital (LUMO) in ICBA lies 0.17 eV higher than that of PCBM, which makes it possible to increase the no-load voltage of the system. The conversion of sunlight into electricity in OPVs with bulk heterojunction can be subdivided into three main stages: light absorption, generation of excitons and their diffusion to the donor/acceptor interface, decay of excitons, and movement of charges to the corresponding electrodes (where they enter the external circuit) [10].

Various approaches are used to improve the morphology of the active layer of organic solar cells with bulk heterojunction: choice of solvent, selection of the optimal mixture concentration and composition, thermal annealing, etc. [11]. In order to achieve higher effectiveness of bulk heterojunction, one needs to consider the stage of exciton dissociation [12], which depends on molecular packing at the interface, in more detail. Thus, the effectiveness of bulk heterojunction of OPVs can be optimized by controlling the morphology of donor–acceptor interface boundaries in the active layer during film formation. In order to achieve this objective, one needs to understand the process of structure formation in polymer–fullerene mixtures. Many studies currently focus on investigating the effect of the active layer morphology on the functionality of OPVs; however, the formation of the nanostructure during film formation has been poorly studied.

In this work, we studied the formation of bulk heterojunction in P3HT : PCBM and P3HT : ICBA films during solvent evaporation. At the first stage we used X-ray diffraction in grazing incidence (GIXD) geometry to study the P3HT mixtures with fullerene derivatives. The most intense peak (100) of P3HT was selected for further high time resolution experiments. When conducting in situ studies, X-ray diffraction analysis was combined with measurement of films conductivity. These experiments make it possible to simultaneously study the structure of the mixture using GIXD methods and conductivity measurements.

EXPERIMENTAL

Materials and Preparation

P3HT with molecular weight of 44.900 g/mol and regioregularity of over 98% was synthesized by the Macromolecular Chemistry Group (the University of Wuppertal, Germany); PCBM (purity over 99.5%) and ICBA (purity over 99%) were purchased from Solenne BV. The solutions of the P3HT : PCBM and P3HT : ICBA mixtures at a 50 : 50 weight ratio with concentration of 5 mg/mL were prepared in $CHCl_3$ and *p*-xylene on a magnetic stirrer at 60°C for 1 h. Glass substrates (18 × 18 mm^2) were cleaned in an ultrasonic bath with Hellmanex II solution and then in 2-propanol and acetone for 20 min, followed by washing with distilled water. For ex situ experiments, 0.02 mL solution drops were deposited on the cleaned glass substrates and covered with glass caps to provide slow drying. For in situ studies, the electrodes were deposited on a coating by thermal evaporation of gold onto a mask with channels 0.5, 1, and 2 mm long and 2 mm wide.

Experimental Procedures

The experiment was carried out at the beamline BL09 of the DELTA synchrotron (Dortmund, Germany) using the GIXD method [13]. Radiant energy was 15.2 keV (wavelength, 0.82 Å); the angle of incidence was 0.1°. The experimental X-ray diffraction patterns were recorded on a PILATUS-100K high-speed detector system. The data in reciprocal space were given in coordinates of the absolute value of the scattering vector [14]. A constant voltage of 10 V was applied to gold electrodes on a Keithley 2400 SourceMeter instrument controlled by LabView package. The entire experiment was conducted in atmosphere of helium and recorded using a camera located directly in the measurement station.

RESULTS AND DISCUSSION

Figure 1 shows the 2D-XRD patterns recorded for film samples from the P3HT : PCBM (left-hand side) and P3HT : ICBA (right-hand side) mixtures. All the XRD patterns contain broad peaks belonging to PCBM. It is believed that fullerenes form aggregates giving rise to small randomly oriented domains. Furthermore, relatively narrow oriented reflections (*h*00) and (020) in the P3HT cell are observed. It was demonstrated for the lattice cell of pure P3HT that reflection (100) corresponds to the distance between the layers formed by side chains, while the (020) peak is indicative of thiophene nuclei (the so-called π–π stack-

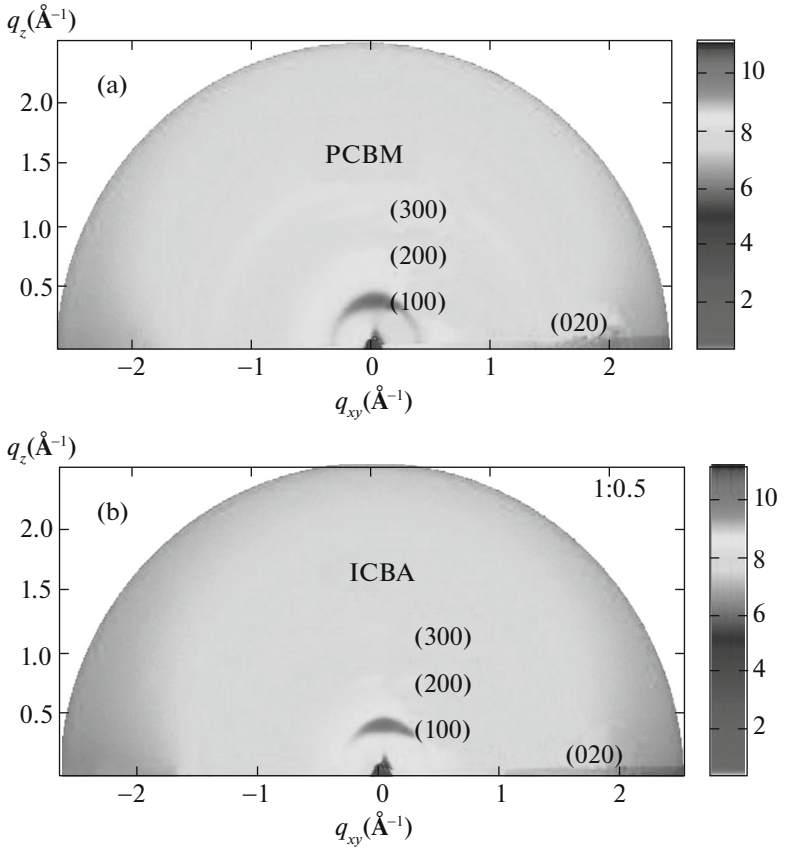

Fig. 1. X-ray diffraction patterns of the (a) P3HT : PCBM and (b) P3HT : ICBA mixtures.

ing) [15]. The interplanar spacing for the P3HT : PCBM (16.15 Å) and P3HT : ICBA (16.21 Å) samples is somewhat smaller than the corresponding value for the (100) peak of the crystalline structure of P3HT (16.62 Å), which probably attests to slight compression of hexyl chains in the mixtures with respect to pure polymer matrix. Thus, a conclusion can be drawn from the analysis of 2D-XRD patterns that side hexyl chains are oriented almost normally with respect to the substrate, while the π-π stacking is mainly oriented along the film surface. The literature data indicate that the interlayer distance (100) in P3HT : PCBM mixtures varies within a broad range from 15.5 to 16.6 Å depending on preparation conditions [16, 17];

Calculated characteristic domain size for the P3HT : PCBM and P3HT : ICBA samples

Parameter	Sample	
	P3HT : PCBM	P3HT : ICBA
Size of acceptor domains (nm)	4.10 (0.15)	1.86 (0.08)
Size of polymer domains in the {100} direction (nm)	11.02 (0.47)	10.36 (0.44)

the position of the π–π stacking peak remains virtually unchanged. Interestingly, the intensity of the ICBA peak for the mixture film is much lower, which indicates that ICBA is more compatible with the polymer. This increases the probability of formation of a continuous interface boundary between the donor and acceptor, which is required to ensure effective exciton decay in bulk heterojunction [18].

Crystal size, one of the important parameters for characterizing the morphology of semicrystalline polymers, was calculated on the nanoscale to obtain information about the 3D structure of the film. Crystal size was calculated using the Selyakov–Sherrer equation [13]; the (100) peak was used for P3HT and the peaks with Q = 1.4 and 1.31 Å^{-1} were used for PCBM and ICBA, respectively (table). Table shows that the half-width of the peak for PCBM (~0.14 Å^{-1}) is twice as high as that of ICBA (~0.32 Å^{-1}). Since a decline in crystal size increases the width of the diffraction peak, the size of P3HT domains turns out to be almost twice as high as that of ICBA domains. The calculated crystallite size of P3HT in the (100) direction is virtually identical for both mixtures (table).

The difference between the values measured in this study and the findings of Wu et al. can be caused by

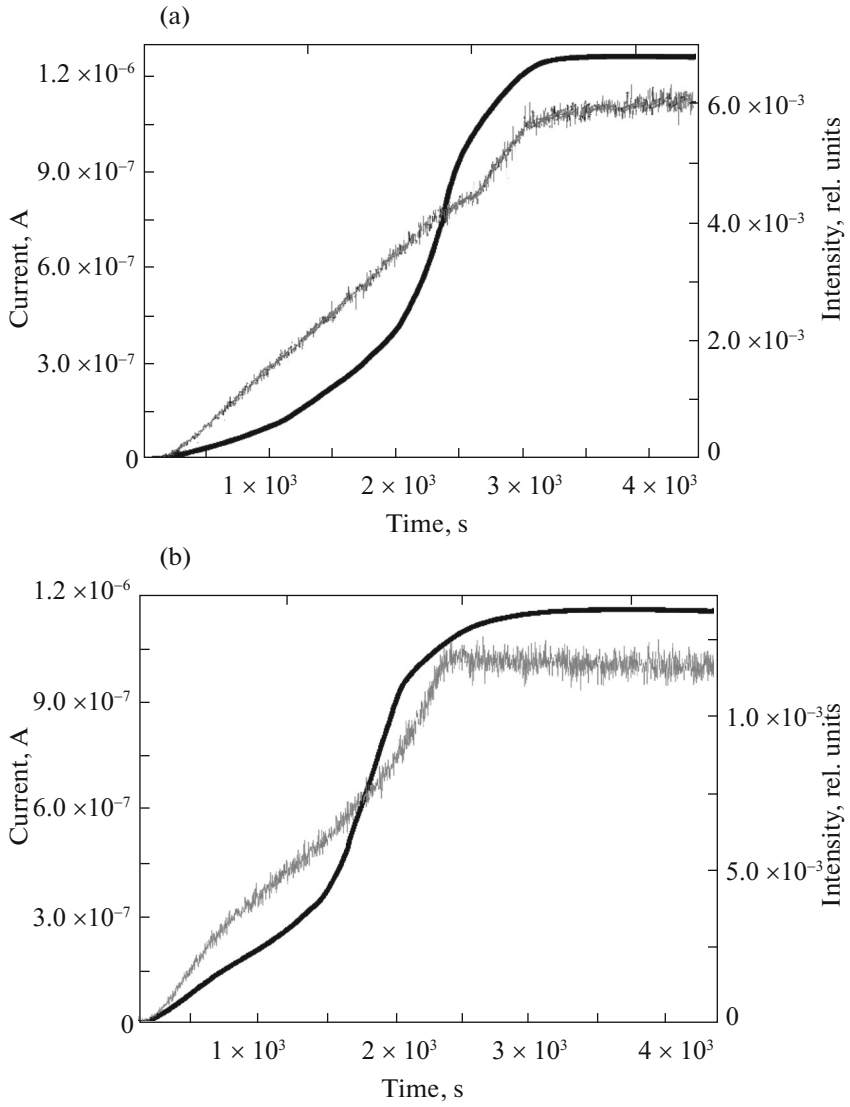

Fig. 2. Time dependence of the current (smooth curve) and intensity of the (100) peak in (a) P3HT : PCBM and (b) P3HT : ICBA films during crystallization.

annealing of the P3HT : PCBM mixture film, which abruptly increases the degree of crystallinity of the mixture [17]. Zhokhavets et al. reported that the minimum crystal size of P3HT in the (h00) direction is 9.2 nm when the P3HT : PCBM film based on the mixture prepared by spin coating is used [19]. Liu et al. used the same mixture and found that the *d*-spacing of (100) for P3HT was equal to 16.7 Å and the corresponding domain size was 11.2 nm, which is close to our results [20]. The small difference between P3HT grain size in two film samples is likely to arise from the fact that ICBA prevents growth of P3HT crystals.

In order to verify this hypothesis, we conducted an in situ experiment and thoroughly analyzed the formation of both films. A drop of the solution of the donor–acceptor mixture was deposited on the substrate between the source and drain electrodes in the very beginning of the experiment. We used *p*-xylene instead of $CHCl_3$ in this experiment, since it takes longer for it to evaporate; hence, the film formation process can be studied with better time resolution. The intensity of the (100) peak of P3HT was found during the experiment simultaneously with the current running between the source and the drain at a constant voltage (10 V) during film formation in the atmosphere of helium.

Figure 2 shows changes in the intensity of the (100) peak of P3HT in the P3HT : fullerene film during film formation vs. changes in current. We demonstrated in our previous studies that current increases linearly with solvent evaporation, reaches its maximum before complete evaporation, and quickly decreases afterwards. It can be assumed that the high degree of crystallinity of the polymer observed in the dried film of

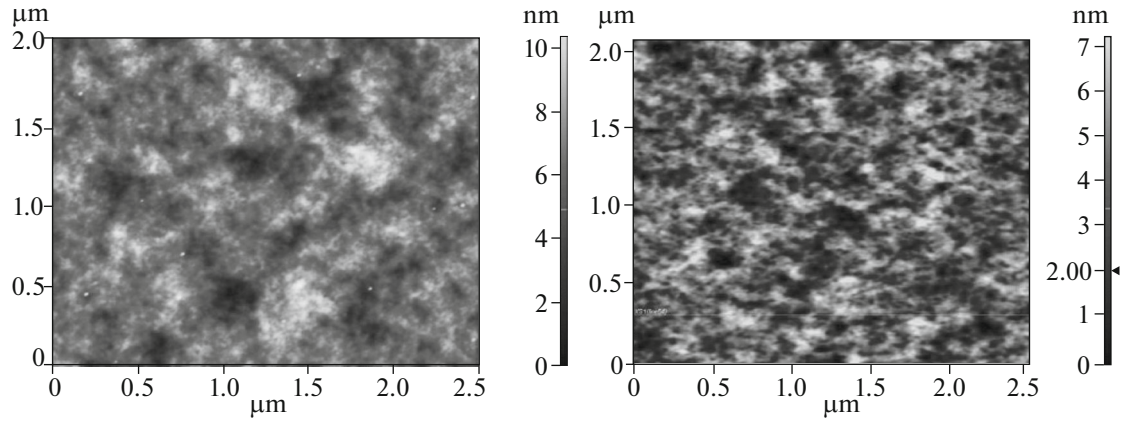

Fig. 3. AFM (topographic) image of the film prepared from the P3HT : PCBM (left-hand side) and P3HT : ICBA (right-hand side) mixtures.

pure P3HT is not the key factor for ensuring the high conductivity of the film. The interaction between domains and their percolation play a crucial role in it.

A two-step increase in current is observed for the P3HT/PCBM film (Fig. 2a); it corresponds to the two-step dependence of the degree of crystallinity (the intensity becomes constant and then increases until it reaches final value). This demonstrates that PCBM molecules are intercalated in the amorphous regions of the polymer at the drying stage, when polymer chains are still highly mobile. This fact once again demonstrates that the two components are mutually soluble. Similar conclusions were drawn upon the assumption that PCBM impedes the formation of π–π stacking in P3HT only when its ratio reaches 1 : 1 [21]. The two-step growth may indicate that crystalline P3HT domains formed at the first stage stimulate the more effective phase segregation of the donor and acceptor in the mixture. The second stage of P3HT crystallization and PCBM aggregation are stimulated by removing PCBM molecules from the crystallizing polymer regions.

Figure 2b shows the results of similar studies for the P3HT : ICBA films. The intensity of the (100) peak increases and current rises linearly from the moment when a drop is deposited on the moment when the maximum is reached in the solid state; the highest conductivity values are observed in the solid state. This fact demonstrates that, due to the better compatibility of the P3HT and ICBA components, the latter forms smaller domains, which impede polymer crystallization during the evaporation of the solvent to a lesser extent.

The differences in crystallization kinetics of the components can be attributed to the difference in the molecular structures of acceptors. Crystalline domains play a crucial role in transport properties of both mixtures, since the formation of ordered domains starts at the final stage of drying; both mixtures exhibit maximum conductivity in the solid state.

In order to obtain a better understanding of the differences in film structure, we studied surface nanotopography. Figure 3 shows the AFM images of the films of P3HT : PCBM and P3HT : ICBA mixtures prepared by spin coating. The AFM images show the identical morphologies at the microscale for both mixtures; neither PCBM nor ICBA aggregates were detected in the structure of annealed films. Root-mean-square roughness (ρ_{rms}) was calculated for both films as a quantitative parameter of the film surface topography. The analysis showed that the P3HT:PCBM film is characterized by smooth surface with $\rho_{rms} = 0.3$ nm and the mean peak height (ρ_{P2V}) = 2.6 nm. The phase-segregated surface with high roughness ($\rho_{rms} = 0.5$ nm and $\rho_{P2V} = 4.4$ nm) is observed for the P3HT:ICBA mixture. Good dispersion of PCBM in the polymer can be achieved by the rapid evaporation of the solvent during quenching and during spin coating when a volatile solvent is used. The comparison of the domain size of acceptors determined by XRD analysis and AFM images confirms that the ICBA-based mixtures tend to form smaller domains (up to 8.5 nm in size), while the PCBM-based mixtures form larger domains (up to 12 nm in size).

CONCLUSIONS

We have conducted a comparative study of two active layers for polymer solar cells based on thin films of the P3HT : PCBM and P3HT : ICBA mixtures. The films prepared at room temperature have an ordered P3HT structure with layers parallel to the substrate and the π–π stacking mainly oriented along the film surface. The P3HT : PCBM mixture is characterized by stronger phase segregation of the components than the P3HT : ICBA film. This result is confirmed by in situ studies of P3HT crystallization process in

films coupled with current measurements in field-effect transistor geometry. Despite the difference in the film formation process, the current reaches its maximum simultaneously with reaching the ultimate degree of crystallinity of P3HT in both cases. The AFM and GIXD data obtained on solid films demonstrate that P3HT : ICBA films tend to form smaller domains, which is preferable for efficient exciton decay at the interface boundary. The study demonstrates that the advantage of the P3HT : ICBA-based systems over those based on P3HT : PCBM in terms of their efficiency is not related to the degree of crystallinity of the polymer but mostly depends on domain size. The percolating network of the donor and acceptor phases can be more efficiently formed in films due to the small domains, providing the transport of charge carriers to the electrodes. On the contrary, it would be reasonable to assume that the formation of large P3HT crystallites in the mixture with PCBM will increase the probability of electron–hole recombination, thus reducing the fill factor (FF), short circuit current (J_{sc}), and the energy conversion coefficient. The obtained results deppens in understanding of the structure formation process in the active layer of organic photovoltaic devices and helps to effectively select the donor and acceptor compounds depending on their compatibility.

ACKNOWLEDGMENTS

This work was supported by the program "Research and Development in Priority Areas of Development of the Russian Scientific and Technological Complex for 2014–2020" (agreement code RFMEFI57414X0097).

REFERENCES

1. C. J. Brabec, S. Gowrisanker, J. J. M. Halls, D. Laird, S. J. Jia, and S. P. Williams, Adv. Mater. **22**, 3839–3856 (2010).
2. U. Irfan and C. Wire, Sci. Am., Oct. 6 (2011).
3. E. Bundgaard and F. C. Krebs, Solar Energy Mater. Solar Cells **91**, 954–985 (2007).
4. T. Agostinelli, S. Lilliu, J. G. Labram, M. Campoy-Quiles, M. Hampton, E. Pires, et al., Adv. Funct. Mater. **21**, 1701–1708 (2011).
5. A. L. Ayzner, D. D. Wanger, C. J. Tassone, et al., J. Phys. Chem. C **112** (48), 18711–18716 (2008).
6. L. Biniek, S. Fall, C. L. Chochos, D. V. Anokhin, D. A. Ivanov, N. Leclerc, P. Lévêque, and T. Heiser, Macromolecules **43**, 9779–9786 (2010)
7. V. Gernigon, P. Leveque, F. Richard, N. Leclerc, C. Brochon, C. Braun, S. Ludwigs, D.V. Anokhin, D. A. Ivanov, G. Hadziioannou, and T. Heiser, Macromolecules **46** (22), 8824–8831 (2013)
8. B. Tremolet de Villers, C. J.Tassone, S. H. Tolbert, et al., J. Phys. Chem. **113** (44), 18978–18982 (2009).
9. M. Ahmadi, K. Mirabbaszadeh, and M. Ketabchi, Electron. Mater. Lett. **9** (6), 729–734 (2013).
10. Y.-H. Lin et al., Org. Electron. **13**, 2333–2341 (2012)
11. M. Al-Ibrahim, O. Ambacher, S. Sensfuß, and G. Gobsch, Appl. Phys. Lett. **86** (20), 201120/1–201120/3 (2005).
12. Y. Carrillo, R. Kumar, M. Goswami, B. Sumpter, et al., Phys. Chem. Chem. Phys. **15**, 17873–17882 (2013).
13. M. Birkholz, *Thin Film Analysis by X-Ray Scattering* (Wiley-VCH, 2006).
14. J. R. May, C. Gentilini, D. E. Clarke, Y. I. Odarchenko, D. V. Anokhin, D. A. Ivanov, K. Feldman, P. Smith, and M. M. Stevens, RSC Adv. **4**, 2096–2102 (2014).
15. J. Als-Nielsen and D. McMorrow, *Elements of Modern X-Ray Physics* (Wiley, 2001).
16. T. S. Shabi, S. Grigorian, M. Brinkmann, et al., J. Appl. Polym. Sci. **125**, 2335–2341 (2012).
17. F.-C. Wu, Y.-C. Huang, H.-L. Cheng, W.-Y. Chou, and F.-C. Tang, J. Phys. Chem. C **115** (30), 15057 (2011).
18. D. Gao, B. Djukic, W. Shi, C. R. Bridges, L. M. Kozycz, and D. S. Seferos, J. Phys. Chem. **5**, 8038–8043 (2013)
19. U. Zhokhavets, T. Erb, H. Hoppe, G. Gobsch, and N. S. Sariciftci, Thin Solid Films **496**, 679–682 (2006).
20. H. Liu, D. Chang, W. Chiu, S. Rwei, and L. Wang, J. Mater. Chem. **22**, 15586–15590 (2012).
21. M. Sanyal, B. Schmidt-Hansberg, M. F. G. Klein, C. Munuera, A. Vorobiev, A. Colsmann, P. Scharfer, U. Lemmer, W. Schabel, H. Dosch, and E. Barrena, Macromolecules **44**, 3795–3800 (2011).

Translated by D. Terpilovskaya